Physica Scripta. Vol. 45, 159–162, 1992.

Alpha Destabilization of the TAE Mode using a Reduced Gyrofluid model with Landau Closure*

D. A. Spong, B. A. Carreras, C. L. Hedrick, N. Dominguez, L. A. Charlton,† P. J. Christenson§ and J-N. Leboeuf

Oak Ridge National Laboratory, Oak Ridge, Tennessee 37831-8071

Received September 12, 1991; accepted October 24, 1991

Abstract

A reduced MHD fluid model for the unstable toroidicity-induced shear Alfvén eigenmode (TAE) is described. This consists of four coupled time evolution equations for the poloidal magnetic flux, toroidal component of vorticity, energetic particle density and parallel flow velocity, which are solved numerically using the three-dimensional initial value code FAR in toroidal geometry. The TAE mode is readily excited and exhibits similar scalings as have been predicted analytically.

1. Introduction

The viability of an ignited deuterium-tritium (D-T) fusion device depends on adequate confinement of the fusion-produced alpha particles through slowing-down time scales. However, energetic plasma components, such as 3.5 MeV alphas, are predicted to couple with and destabilize discrete shear Alfvén gap modes. This can result in new instabilities that are unique to ignited tokamaks and would not be apparent in present experiments. An example is the toroidicity-induced shear Alfvén eigenmode (TAE) mode, which is located in the spectral gaps between the sher Alfvén continua [1, 2]. Passing alpha particles with parallel velocities near the TAE phase velocity can resonantly couple to these discrete gap roots and drive them unstable by transferring the free energy in the alpha density gradient [3–7]. There has been considerable interest in this instability because of its sizable growth rate and global mode structure. Several recent theoretical models have predicted its presence in ignited tokamaks such as the Burning Plasma Experiment (BPX, formerly CIT) and the International Thermonuclear Experimental Reactor (ITER) [5, 6]. Also, numerical orbit-following calculations have shown fast alphas can rapidly be removed from the plasma in the presence of a linear TAE mode structure long before they thermalize, [8] thus impacting requirements for a self-sustaining ignited state. In addition, experiments in beam-heated tokamaks operated at low magnetic fields (such that $v_{\text{beam}} > v_{\text{Alfvén}}$) have recently demonstrated the existence of fluctuations in the frequency range appropriate to the TAE mode [9, 10].

The existing theory of the TAE instability has been primarily based on the use of kinetic quadratic forms [3–7]. These have been either minimized numerically [4, 6] or evaluated analytically [3, 5, 7] by using the stable discrete gap eigenmode without alphas as a trial function. The purpose of this paper is to discuss an alternative approach: a set of fluidlike time evolution equations that contain the gap mode and can be solved with existing magnetohydrodynamic (MHD) initial value codes. A Landau fluid model with consistent closure relations [11, 12] is used for the alphas and a reduced MHD model for the background plasma. Also, the effects of background pressure, finite ion Larmor radius, and Landau damping on the background ions and electrons are neglected. This model can be generalized in these areas, and such improvements are currently under way.

2. Basic equations

The model is based on toroidal geometry with R the major radius, φ the toroidal angle, and z the vertical coordinate along the symmetry axis. We assume the usual tokamak ordering of $B_{\text{poloidal}}/B_{\text{toroidal}} \ll 1$ and eliminate the fast Alfvén wave. The fluid equations that result from keeping the φ components of Ampére's law, Faraday's law and the perpendicular component (to φ) of the momentum balance equation are:

$$J_\varphi = \mu_0 R \nabla_\perp \cdot \left(\frac{1}{R^2}\nabla_\perp \psi\right), \tag{1}$$

$$\frac{\partial \psi}{\partial t} = \hat{b} \cdot \nabla \phi, \tag{2}$$

$$\rho_{\text{ion}} \frac{d\boldsymbol{v}_\perp}{dt} = \boldsymbol{J} \times \boldsymbol{B} - \sum_{j=\text{th},\alpha} \nabla_\perp p_j \tag{3}$$

with $\psi = -RA_\varphi$ and $\hat{b} = \boldsymbol{B}/B$.

Here ϕ is the electrostatic potential, μ_0 is the free space permeability, and ψ is the poloidal magnetic flux function. The energetic alpha component is assumed to enter only through the pressure gradient term in eq. (3). We next multiply eq. (3) by R/B_φ, take the curl of this equation, keep only the φ component, and transform to straight-field-line coordinates. This results in:

$$\frac{\partial U}{\partial t} = \nabla_\parallel J_\varphi + \sum_j \frac{\beta_{j0}}{2\varepsilon^2}\left[\frac{1}{r}\frac{\partial}{\partial\theta}\left(\frac{R^2}{F}\right)\frac{\partial \tilde{p}_j}{\partial r} - \frac{\partial}{\partial r}\left(\frac{R^2}{F}\right)\frac{1}{r}\frac{\partial \tilde{p}_j}{\partial\theta}\right], \tag{4}$$

* Research sponsored by the Office of Fusion Energy, U.S. Department of Energy, under contract DE-AC05-84OR21400 with Martin Marietta Energy Systems, Inc., also under appointment to the Magnetic Fusion Energy Technology Fellowship program administered by Oak Ridge Associated Universities for DOE.

† Computing and Telecommunications Division, Martin Marietta Energy Systems, Inc., Oak Ridge, Tennessee 37831.

§ Permanent address: University of Michigan, Nuclear Engineering Department, Ann Arbor, Michigan.

with $F = RB_\varphi$, $\beta_{j0} = \beta$ of species j at magnetic axis, and

$$U = \frac{1}{r}\frac{\partial}{\partial r}\left[\frac{R^4}{F^2}\rho_{\text{ion}}(r) r\left(g^{rr}\frac{\partial\tilde{\phi}}{\partial r} + g^{r\theta}\frac{1}{r}\frac{\partial\tilde{\phi}}{\partial\theta}\right)\right] + \frac{\rho_{\text{ion}}(r)}{r}\frac{\partial}{\partial\theta}\left[\frac{R^4}{F^2}\left(g^{r\theta}\frac{\partial\tilde{\phi}}{\partial r} + g^{\theta\theta}\frac{1}{r}\frac{\partial\tilde{\phi}}{\partial\theta}\right)\right],$$

$$\nabla_\parallel X = \nabla_\parallel^{(0)} X - \frac{\partial X_{\text{eq}}}{\partial r}\frac{1}{r}\frac{\partial\tilde{\psi}}{\partial\theta} + \frac{\partial\tilde{\psi}}{\partial r}\frac{1}{r}\frac{\partial\tilde{X}}{\partial\theta} - \frac{\partial\tilde{X}}{\partial r}\frac{1}{r}\frac{\partial\tilde{\psi}}{\partial\theta};$$

$$\nabla_\parallel^{(0)} X = \left(\frac{\partial}{\partial\varphi} - \frac{1}{q}\frac{\partial}{\partial\theta}\right)X.$$

Here g^{rr}, $g^{r\theta}$, $g^{\theta\theta}$ are the metric elements of our flux surface coordinate system. We have employed the usual reduced MHD normalizations: t is normalized to the poloidal Alfvén time $\tau_{\text{Hp}} = R_0/v_{\text{A0}}$, with v_{A0} the Alfvén velocity at the magnetic axis; ϕ is normalized to a^2B_0/τ_{Hp} and ψ is normalized to a^2B_0, with B_0 the magnetic field at the magnetic axis; the minor radius r is normalized to a; $\tilde{p}_j$ is normalized to the value of the equilibrium pressure of species j at the magnetic axis, p_{j0}; and $\beta_{j0} = 2\mu_0 p_{j0}/B_0^2$.

The alpha component is included in our calculation using a gyrofluid model with Landau closure. This technique was previously developed for the electrostatic η_i mode [11] and has recently been extended to the case of alpha populations coupled to electromagnetic shear Alfvén waves [12]. The basic procedure is to solve the linearized kinetic equation in the normal manner in terms of the plasma dispersion function; this solution is next compared with that resulting when a moments hierarchy is developed from the same kinetic equation. A closure relation is then constructed such that the moments solution is equivalent to the exact kinetic solution if an n-pole approximation is made to the plasma dispersion function.

This technique contains the necessary mechanism for exciting the unstable TAE mode since this occurs via inverse Landau damping through the alpha component. A set of moment equations with consistent Landau closure has been developed [12] for alphas based on a fully electromagnetic slab model, using a two-pole approximation to the plasma dispersion function and assuming constant drift velocity (i.e., evaluated at the thermal velocity). Use of a two-pole approximation implies that two fluid equations will be required for the alphas. These are the time evolution of the alpha density and parallel flow velocity. Converting the density equation to a pressure equation (the alpha temperature has been assumed constant here) and using the same normalized units as discussed above results in the following equations:

$$\frac{\partial\tilde{p}_\alpha}{\partial t} = -\frac{\hat{\omega}_{\text{d}\alpha}\partial\tilde{p}_\alpha}{r\ \partial\theta} + \frac{\text{d}p_{0\alpha}}{\text{d}r}\frac{1}{r}\frac{\partial\phi}{\partial\theta} - p_{0\alpha}\nabla_\parallel\tilde{v}_{\parallel\alpha} - \frac{\varepsilon^2\hat{\omega}_{c\alpha}p_{0\alpha}}{\hat{v}_{\text{th}\alpha}^2}\frac{\hat{\omega}_{\text{d}\alpha}}{r}\frac{\partial\phi}{\partial\theta} + \hat{D}_{\text{p}_\alpha}\nabla_\perp^2\tilde{p}_\alpha \tag{5}$$

$$\frac{\partial\tilde{v}_{\parallel\alpha}}{\partial t} = -\frac{\hat{\omega}_{\text{d}\alpha}}{r}\frac{\partial\tilde{v}_{\parallel\alpha}}{\partial\theta} - \left(\frac{\pi}{2}\right)^{1/2}\hat{v}_{\text{th}\alpha}|\nabla_\parallel|\tilde{v}_{\parallel\alpha} - \frac{\hat{v}_{\text{th}\alpha}^2}{p_{0\alpha}(r)}\nabla_\parallel\tilde{p}_\alpha + \frac{\varepsilon^2\omega_{c\alpha}\omega_{*\alpha}}{r}\frac{\partial\psi}{\partial\theta} \tag{6}$$

where

$$\hat{\omega}_{\text{d}\alpha} = -\frac{\hat{v}_{\text{th},\alpha}^2}{\varepsilon^2\hat{\omega}_{c\alpha}}R\frac{\partial R^{-1}}{\partial r},\quad \hat{\omega}_{c\alpha} = \Omega_{c\alpha}\tau_{\text{Hp}},$$

$$\varepsilon = a/R_0,\quad \hat{v}_{\text{th},\alpha} = v_{\text{th},\alpha}/v_{\text{A0}},$$

$$\hat{\omega}_{*\alpha} = \frac{\hat{v}_{\text{th},\alpha}^2}{\varepsilon^2\hat{\omega}_{c\alpha}}\left[\frac{1}{n_{0\alpha}}\frac{\text{d}n_{0\alpha}}{\text{d}r}\right],\quad \hat{D}_{p_\alpha} = D_{\text{p}_\alpha}\tau_{\text{Hp}}/a^2,$$

$$v_{\text{th},\alpha} = \sqrt{T_\alpha/M_\alpha}$$

Here $\Omega_{c\alpha}$ is the α cyclotron frequency, T_α is the alpha temperature, and the perturbed alpha pressure and parallel flow velocity have been normalized to the equilibrium pressure and the Alfvén speed at the magnetic axis (v_{A0}), respectively. The $|\nabla_\parallel|$ operator has a simple interpretation only for the case in which φ and θ are Fourier analyzed, in which case it is the absolute value of the parallel wavenumber. A small amount of diffusion is included in the alpha pressure evolution equation for numerical reasons; this is at a level where it does not have a significant effect on the answers obtained. Equations (1), (2), (5) and (6) then complete our system of time evolution equations.

This model is solved in toroidal geometry with the three-dimensional (3-D) initial value code FAR [13], which evolves the four scalar fields ψ, U, $\tilde{p}_\alpha$, $\tilde{v}_{\parallel\alpha}$ using an implicit algorithm. All quantities are expanded in Fourier harmonics in φ and θ and discretized on a radial grid. The time evolution is followed until an asymptotic, linear, exponentially growing state is achieved.

3. Results

The strength of the alpha-destabilized TAE mode is directly influenced both by the level of alpha pressure and its gradient, since the driving terms scale with these parameters. Scaling of the growth rate with $p_{\alpha0}^{-1}|\text{d}p_{\alpha0}/\text{d}r|$ and $\beta_{\alpha0}$ is thus of interest for validating the present model against analytic growth rate predictions and for comparison with experiment. Another characteristic feature of the TAE mode is that its real frequency, ω_{real}, should be relatively fixed at that of the original, resonant discrete shear Alfvén mode. This can be approximately determined [5] by the crossing point of the two adjacent cylindrical continua and is $\omega_{\text{real}}\tau_{\text{Hp}} = n/(2m+1) = \frac{1}{3}$ for $n = 1$, $m = 1$. Such roots become readily apparent in solving our system of evolution equations. We assume an energetic species equilibrium profile $p_{\alpha0}(r) = \exp(-r^2/L_\alpha^2)$, take a flat ion density profile, and include the modes $n = 1$, $m = (0$ to $6)$. Typical scalings of the real frequency and growth rate vs. the alpha pressure gradient parameter, L_α/a obtained from the numerical results are displayed in Fig. 1. The parameters $(T_\alpha/M_\alpha)^{1/2} = 1.05v_{\text{A0}}$, $\beta_{\alpha0} = 0.004$, $\hat{D}_{\text{p}\alpha} = 10^{-4}$, and $\hat{\omega}_{c\alpha} = 100$ are used. The equilibrium is numerically computed with $\varepsilon = 0.25$ and zero β is the background plasma. The q profile is

$$q(r) = q_0\left[1 + \left(\frac{r}{r_0}\right)^{2\lambda}\right]^{1/\lambda},$$

with $q_0 = 1.05$, $\lambda = 1$, $r_0 = 0.956$ and $q(1) = 2.2$. These simplified profiles are chosen since they result in only a single TAE gap formed by coupling of the $m = 1$ and $m = 2$ modes, as is typically assumed in the analytical treatments. The other parameters we have chosen are fairly typical of ignited devices, but are not intended to correspond to any

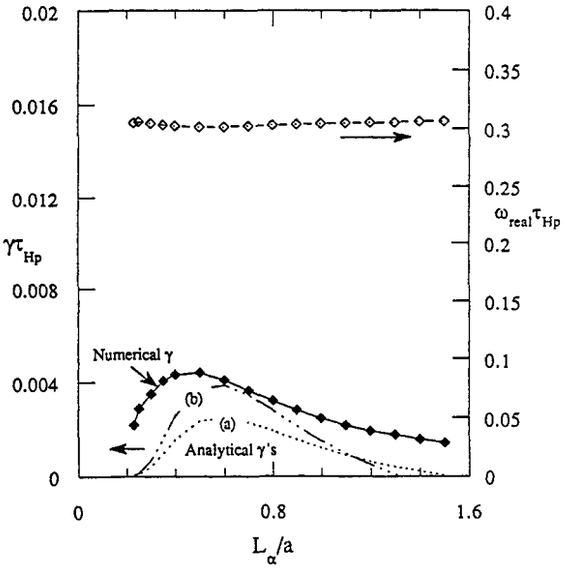

Fig. 1. Dependence of real frequency and growth rate on alpha pressure profile [for $\beta_{\alpha 0} = 0.004$, $\varepsilon = 0.25$, $\hat{D}_{p\alpha} = 10^{-4}$, $(T_\alpha/M_\alpha)^{1/2} = 1.05 v_{A0}$, $\hat{\omega}_{c\alpha} = 100$, ρ_{ion} = constant].

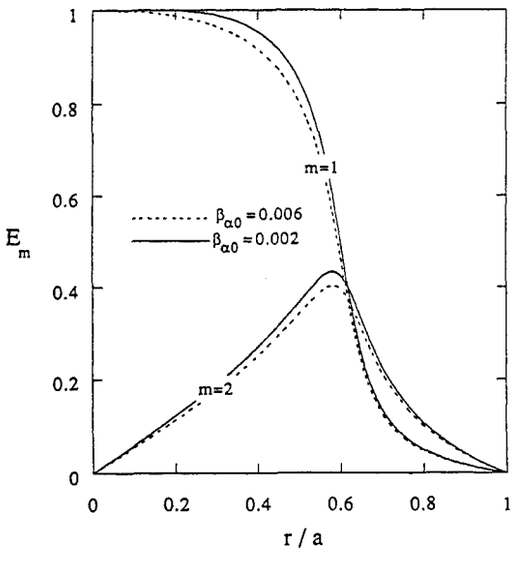

Fig. 2. Typical radial dependence of poloidal electric field eigenfunctions (for $\beta_{\alpha 0} = 0.002$ and 0.006, $\varepsilon = 0.25$).

particular device. Figure 1 indicates the real frequency is relatively constant near $\omega_{real}\tau_{Hp} \approx 0.3$, as expected. The growth rate first increases as the gradient steepens and then decreases. The dropoff for $L_\alpha/a < 0.5$ is due to the fact that the maximum gradient region of the $p_{\alpha 0}(r)$ profile is shifting inward from the TAE gap location [which is at $r_{gap} = 0.63$, i.e., for our q profile $q(r_{gap}) = (m + \frac{1}{2})/n = 1.5$]. For $L_\alpha/a > 0.5$ the profile is broadening, causing the local gradient at the gap location to decrease and lowering the growth rate. Similar scaling is seen in the analytic growth rate estimates with curve (a) corresponding to Ref. [3] and curve (b) to Ref. [7]. Using our pressure profile and taking $n = 1$, the result of Ref. [3] can be written as:

$$\frac{\gamma}{\omega_{real}} = \frac{9}{4}\beta_\alpha\left[\frac{m(T_\alpha/M_\alpha)}{\omega_{real}\Omega_{c\alpha}L_\alpha^2} - 1\right]g(x),$$

with $g(x) = x(1 + 2x^2 + 2x^4)e^{-x^2}$ and $x = v_A/\sqrt{2T_\alpha/M_\alpha}$ while that of Ref. [7] is:

$$\frac{\gamma}{\omega_{real}} = \frac{9\sqrt{\pi}}{8}\beta_\alpha\left(\frac{3rr_{L\theta}}{L_\alpha^2 x} - 1\right)[g(x) + g(x/3)].$$

Here $r_{L\theta}$ is the alpha poloidal gyroradius. Since the numerical calculation includes more poloidal modes and takes into account the full global radial structure, it should not be expected to precisely agree; however, both results do indicate similar scaling. The elevated growth rate of the numerical calculation at the higher values of L_α/a and lack of a marginal point is likely due to coupling to higher order poloidal modes (up to $m = 6$ is included) for which the alpha Landau growth term ($\propto \omega_{*\alpha}$) still exceeds the alpha Landau damping term ($\propto \omega_{real}$). In Fig. 2, we plot the radial structure of the poloidal electric field for two values of $\beta_{\alpha 0}$. These are quite similar to the gap eigenfunctions given in Ref. [3], except for minor differences due to the slightly different q profile we use here. The radial mode structure appears to be relatively insensitive to variations in $\beta_{\alpha 0}$ over the ranges considered here. Next, in Fig. 3 we show the scaling of the real frequency and the growth rate with the energetic species $\beta_{\alpha 0}$ (for $L_\alpha/a = 0.35$). For comparison, the analytically predicted growth rates of Refs [3] and [7] for a Maxwellian energetic species distribution (without electron Landau damping) are shown by the remaining curves with (a) corresponding to Ref. [3] and curve (b) to Ref. [7]. All calculations indicate a linear scaling with $\beta_{\alpha 0}$ and a stability threshold at $\beta_{\alpha 0} = 0$ (which will move to a finite value of $\beta_{\alpha 0}$ if background ion and electron Landau damping are included).

Finally, we examine the scaling with respect to the thermal velocity of the alpha component. In Fig. 4 numerically obtained growth rates are plotted as $(2T_\alpha/M_\alpha)^{1/2}/v_{A0}$ varies from about 0.3 up to 2. For these runs we have taken $\beta_{\alpha 0} = 0.004$, $L_n/a = 0.4$ and again compared with analytic results from Refs [3] (curve (a)) and [7] (curve (b)). As may be seen, the numerical growth rates are higher, although the scaling is similar, especially at the larger values of $(2T_\alpha/M_\alpha)^{1/2}/v_{A0}$. For lower values of $(2T_\alpha/M_\alpha)^{1/2}/v_{A0}$, the numerical growth rates do not drop off as fast as the anlytic

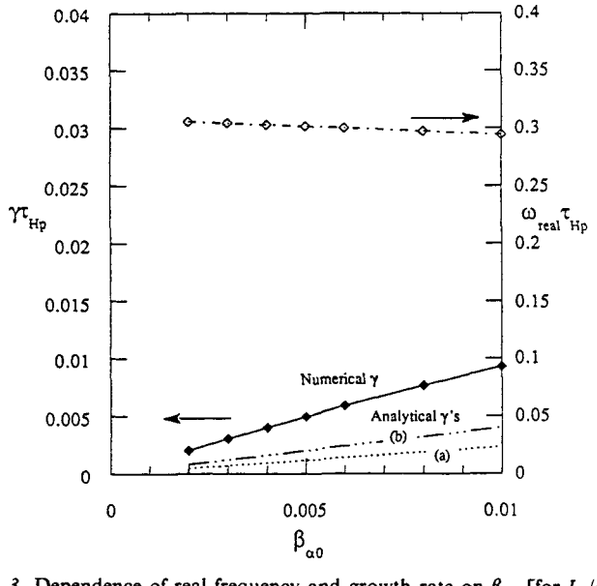

Fig. 3. Dependence of real frequency and growth rate on $\beta_{\alpha 0}$ [for $L_\alpha/a = 0.35$, $\varepsilon = 0.25$, $\hat{D}_{p\alpha} = 10^{-4}$, $(T_\alpha/M_\alpha)^{1/2} = 1.05 v_{A0}$, $\hat{\omega}_{c\alpha} = 100$, ρ_{ion} = constant].

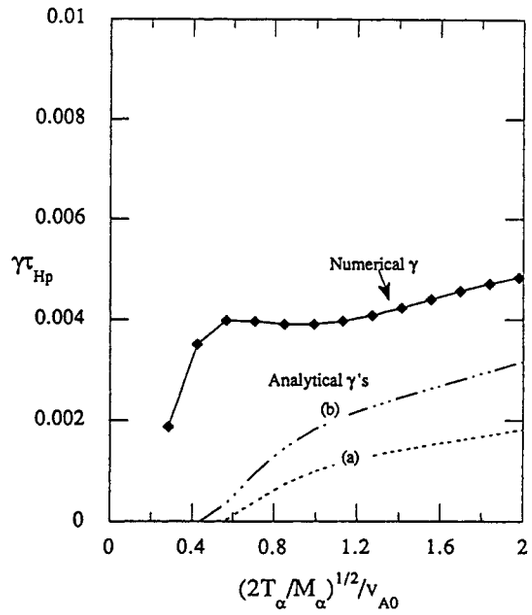

Fig. 4. Dependence of growth rate on mean alpha energy [for $\beta_{\alpha 0} = 0.004$, $L_\alpha/a = 0.35$, $\varepsilon = 0.25$, $\hat{D}_{p\alpha} = 10^{-4}$, $\hat{\omega}_{c\alpha} = 100$, ρ_{ion} = constant].

ones. This is likely to be due again to the larger number of poloidal modes included in the numerical calculation; the higher m sidebands allow coupling to the hot distribution at lower velocities in the distribution. This feature is partially present in the analysis of Ref. [7] where coupling of the hot species with the first sideband ($m = 2$) is included in addition to the coupling at the fundamental ($m = 1$), which is retained in both analytical calculations [3, 7].

4. Conclusions

A simplified fluid model has been presented for the alpha-destabilized TAE gap mode. Numerical solutions using the existing MHD initial value code FAR [10] have indicated real frequencies and growth rate scalings characteristic of the TAE instability. This opens up a number of new possibilities for study of the gap mode that would be either difficult or impossible using other methods. First of all, the model can be extended to the nonlinear regime if mode coupling and profile relaxation are assumed to be the dominant nonlinearities. Second, in the linear regime, it is relatively easy to include multiple poloidal modes (to check convergence), examine noncircular cross sections, and consider toroidal mode numbers $n > 1$. Also, it is a relatively simple extension to include the background plasma pressure-gradient drive, Landau damping on the background ions and electrons, finite ion FLR, and various dissipative effects (resistivity, viscosity, etc.) in this type of model. Although the latter might be expected to be small for the parameters of ignited devices, they have been shown to significantly modify the nature of the underlying shear Alfvén spectrum [14].

References

1. Kieras, C. and Tataronis, J., J. Plasma Phys., **28**, 395 (1982).
2. Cheng, C. Z., Chen, L. and Chance, M. S., Ann. of Phys. **161**, 21 (1985); Cheng, C. Z. and Chance, M. S., Phys. Fluids **29**, 3695 (1986).
3. Fu, G. Y. and Van Dam, J. W., Phys. Fluids **B1**, 1949 (1989).
4. Cheng, C. Z., Fusion Technol. **18**, 443 (1990).
5. Van Dam, J. W., Fu, G-Y. and Cheng, C. Z., Fusion Technol. **18**, 461 (1990).
6. Cheng, C. Z., see National Technical information Service document No. DE 91000486 (Princeton Plasma Physics Laboratory Report PPPL-2717). Copies may be ordered from the National Technical Information Service, Springfield, Virginia 22161. The price is $15.00 (for 26-50 pages) plus a $3.00 handling fee. All orders must be prepaid.
7. Betti, R. and Freidberg, J. P., 1991 Sherwood Theoretical Meeting, Seattle, Washington.
8. Sigmar, D. J. and Hsu, C. T., invited talk at 1991 Sherwood Theory Meeting, Seattle, Washington.
9. Wong, K. L. and Fonck, R. J. *et al.*, Phys. Rev. Lett. **66**, 1874 (1991).
10. Heidbrink, W. W., Strait, E. J., Doyle, E., Sager, G. and Snider, R., submitted to Nuclear Fusion.
11. Hammet, G. W. and Perkins, F. W., Phys. Rev. Lett. **64**, 3019 (1990).
12. Hedrick, C. L., invited talk at 1991 Sherwood Theory Meeting, Seattle, Washington.
13. Charlton, L., Holmes, J. A., Hicks, H. R., Lynch, V. E. and Carreras, B. A., J. Comput. Phys., **63**, 107 (1986).
14. Appert, K., Collins, G. A., Hellsten, T., Vaclavik, J. and Villard, L., Plasma Phys. Controlled Fusion **28**, 133 (1986).